Antitumor Activity of Plant Cannabinoids with Emphasis on the Effect of Cannabidiol on Human Breast Carcinoma

Alessia Ligresti, Aniello Schiano Moriello, Katarzyna Starowicz, Isabel Matias, Simona Pisanti, Luciano De Petrocellis, Chiara Laezza, Giuseppe Portella, Maurizio Bifulco, and Vincenzo Di Marzo

Endocannabinoid Research Group, Istituto di Chimica Biomolecolare (A.L., A.S.M., K.S., I.M., V.D.M.), and Istituto di Cibernetica (A.S.M., L.D.P.), Consiglio Nazionale delle Ricerche Pozzuoli, Italy; Dipartimento di Biologia e Patologia Cellulare e Molecolare "L. Califano", Università di Napoli "Federico II", Napoli, Italy (S.P., C.L., G.P., M.B.); and Dipartimento di Scienze Farmaceutiche, Università degli Studi di Salerno, Fisciano, Italy (S.P., M.B.)

Received March 25, 2006; accepted May 23, 2006

ABSTRACT

Δ^9-Tetrahydrocannabinol (THC) exhibits antitumor effects on various cancer cell types, but its use in chemotherapy is limited by its psychotropic activity. We investigated the antitumor activities of other plant cannabinoids, i.e., cannabidiol, cannabigerol, cannabichromene, cannabidiol acid and THC acid, and assessed whether there is any advantage in using Cannabis extracts (enriched in either cannabidiol or THC) over pure cannabinoids. Results obtained in a panel of tumor cell lines clearly indicate that, of the five natural compounds tested, cannabidiol is the most potent inhibitor of cancer cell growth (IC_{50} between 6.0 and 10.6 μM), with significantly lower potency in noncancer cells. The cannabidiol-rich extract was equipotent to cannabidiol, whereas cannabigerol and cannabichromene followed in the rank of potency. Both cannabidiol and the cannabidiol-rich extract inhibited the growth of xenograft tumors obtained by s.c. injection into athymic mice of human MDA-MB-231 breast carcinoma or rat v-K-ras-transformed thyroid epithelial cells and reduced lung metastases deriving from intrapaw injection of MDA-MB-231 cells. Judging from several experiments on its possible cellular and molecular mechanisms of action, we propose that cannabidiol lacks a unique mode of action in the cell lines investigated. At least for MDA-MB-231 cells, however, our experiments indicate that cannabidiol effect is due to its capability of inducing apoptosis via: direct or indirect activation of cannabinoid CB_2 and vanilloid transient receptor potential vanilloid type-1 receptors and cannabinoid/vanilloid receptor-independent elevation of intracellular Ca^{2+} and reactive oxygen species. Our data support the further testing of cannabidiol and cannabidiol-rich extracts for the potential treatment of cancer.

The therapeutic properties of the hemp plant, Cannabis sativa, have been known since antiquity, but the recreational use of its euphoric and other psychoactive effects has restricted for a long time research on its possible pharmaceutical application. The isolation of Δ^9-tetrahydrocannabinol (THC), the main psychoactive component of Cannabis (Gaoni and Mechoulam, 1964), opened the way to further investiga-

tions. After the discovery of the two specific molecular targets for THC, CB_1, and CB_2 (for review, see Pertwee, 1997), it became clear that most of the effects of marijuana in the brain and peripheral tissues were due to activation of these two G-protein-coupled cannabinoid receptors. However, evidence is also accumulating that some pharmacological effects of marijuana are due to Cannabis components different from THC. Indeed, C. sativa contains at least 400 chemical components, of which 66 have been identified to belong to the class of the cannabinoids (Pertwee, 1997).

To date, cannabinoids have been successfully used in the treatment of nausea and vomiting (for review, see Robson,

ABBREVIATIONS: THC, Δ^9-tetrahydrocannabinol; CB_1, cannabinoid receptor type-1; CB_2, cannabinoid receptor type-2; TRPV1, transient receptor potential vanilloid type-1; SR141716A, N-(piperidin-1-yl)-5-(4-chlorophenyl)-1-(2,4-dichlorophenyl)-4-methyl-1H-pyrazole-3-carboxamide HCl; SR144528, N-[(1S)-endo-1,3,3-trimethylbicyclo[2.2.1]heptan-2-yl]-5-(4-chloro-3-methylphenyl)-1-(4-methylbenzyl)-1-pyrazole-3-carboxamide; JWH-133, 1,1-dimethylbutyl-1-deoxy-Δ^9-tetrahydrocannabinol; AM251, N-(piperidin-1-yl)-5-(4-iodophenyl)-1-(2,4-di-chlorophenyl)-4-methyl-1H-pyrazole-3-carboxamide; AM630, 6-iodo-2-methyl-1-[2-(4-morpholinyl)-ethyl]-1H-indol-3-yl](4-methoxyphenyl)-methanone; ANOVA, analysis of variance; ROS, reactive oxygen species; RT, reverse transcription; PCR, polymerase chain reaction; GAPDH, glyceraldehyde-3-phosphate dehydrogenase; nt, nucleotide; PBS, phosphate-buffered saline; I-RTX, 5'-iodo-resiniferatoxin; HEK, human embryonic kidney; CBD, cannabidiol; BAPTA-AM, 1,2-Bis(2-aminophenoxy)ethane-N,N,N',N'-tetraacetic acid tetrakis (acetoxymethyl ester).

2005), two common side effects that accompany chemotherapy in cancer patients. Nevertheless, the use of cannabinoids in oncology might be somewhat underestimated since increasing evidence exist that plant, synthetic, and endogenous cannabinoids (endocannabinoids) are able to exert a growth-inhibitory action on various cancer cell types. However, the precise pathways through which these molecules produce an antitumor effect has not been yet fully characterized, also because their mechanism of action appears to be dependent on the type of tumor cell under study. It has been reported that cannabinoids can act through different cellular mechanisms, e.g., by inducing apoptosis, cell-cycle arrest, or cell growth inhibition, but also by targeting angiogenesis and cell migration (for review, see Bifulco and Di Marzo, 2002; Guzman, 2003; Kogan, 2005). Furthermore, the antitumoral effects of plant, synthetic and endocannabinoids can be mediated by activation of either CB_1 (Melck et al., 2000; Bifulco et al., 2001; Ligresti et al., 2003; Mimeault et al., 2003) or CB_2 receptors or both (Sanchez et al., 2001; Casanova et al., 2003; McKallip et al., 2005), and, at least in the case of the endocannabinoid anandamide, by transient receptor potential vanilloid type-1 (TRPV1) receptors (Maccarrone et al., 2000; Jacobsson et al., 2001; Contassot et al., 2004) as well as by noncannabinoid, nonvanilloid receptors (Ruiz et al., 1999). Additionally, cannabidiol has been suggested to inhibit glioma cell growth in vitro and in vivo independently from cannabinoid and vanilloid receptors (Massi et al., 2004; Vaccani et al., 2005).

The main limitation of the possible future use of THC in oncology might be represented by adverse effects principally at the level of the central nervous system, consisting mostly of perceptual abnormalities, occasionally hallucinations, dysphoria, abnormal thinking, depersonalization, and somnolence (Walsh et al., 2003). However, most non-THC plant cannabinoids seem to be devoid of direct psychotropic proprieties. In particular, it has been ascertained that cannabidiol is nonpsychotropic (for review, see Mechoulam et al., 2002; Pertwee, 2004) and may even mitigate THC psychoactivity by blocking its conversion to the more psychoactive 11-hydroxy-THC (Bornheim and Grillo, 1998; Russo and Guy, 2006). Moreover, it has been recently found that systematic variations in its constituents (i.e., cannabidiol and cannabichromene) do not affect the behavioral or neurophysiological responses to marijuana (Ilan et al., 2005). Finally, it has been also shown that, unlike THC, systemic administration to rats of cannabigerol does not provoke poly-spike discharges in the cortical electroencephalogram during wakefulness and behavioral depression (Colasanti, 1990). These and other observations reinforce the concept that at least cannabidiol, cannabigerol, and cannabichromene lack psychotropic activity and indicate that for a promising medical profile in cancer therapy, research should focus on these compounds, which instead have been poorly studied with regard to their potential antitumor effects. By keeping this goal in mind, we decided to investigate the antitumor properties of cannabigerol and cannabichromene. We also screened THC acid and cannabidiol acid and two distinct *Cannabis* extracts (enriched in either cannabidiol or THC), where the presence of nonpsychotropic cannabinoids along with THC has been reported to mitigate the potential side effects of the latter compound in clinical trials (Russo and Guy, 2006).

Materials and Methods

Drugs. All plant cannabinoids, the two cannabinoid acids, and the two *Cannabis* extracts were kindly provided by GW Pharmaceuticals (Wiltshire, UK; Fig. 1). Cannabidiol- and THC-rich extracts contained approximately 70% cannabidiol or THC, respectively, together with lesser amounts of other cannabinoids. The two cannabinoid receptor antagonists, SR141716A and SR144528, were a kind gift from Sanofi-Aventis (Paris, France), whereas methyl-β-cyclodextrin, all of the antioxidant drugs (α-tocopherol, vitamin C, astaxantine), *N*-Acetyl-Asp-Glu-Val-Asp-aldehyde, and BAPTA-AM were purchased from Sigma-Aldrich (St. Louis, MO). The endocannabinoid uptake inhibitor (S)-1'-(4-hydroxybenzyl)-*N*-ethyl-oleoylamide was synthesized as previously described in Ortar et al. (2003). Finally, all of the TRPV1 or cannabinoid receptor agonists and antagonists (capsaicin, resiniferatoxin, arachidonoyl-2-chloro-ethylamide, JWH-133, AM251, AM630) were obtained from Tocris Cookson (Bristol, UK).

Cell Cultures. Cell lines from various origins (MCF-7 and MDA-MB-231 human breast carcinoma cells, DU-145 human prostate carcinoma cells, CaCo-2 human colorectal carcinoma cells, AGS human gastric adenocarcinoma cells, C_6 rat glioma cells, KiMol rat thyroid cells transformed with the v-K-*ras* oncogene, and rat basophilic leukemia cells) were maintained at 37°C in a humidified atmosphere containing 5% CO_2. Media, sera, and subculturing procedures differed from line to line and were according to the information provided in each case by the supplier company (DSMZ, Braunschweig, Germany). Primary cells derived from normal human mammary glands were purchased from Cell Applications, Inc. (San Diego, CA) and cultured as described in the data sheet from the supplier.

Cell Proliferation Assay. Six-well culture plates were incubated at 37°C at a cell density of 5×10^4 cells/well in a humidified atmosphere containing 5% CO_2. Three hours after seeding, vehicle or cannabinoids at different concentrations were added to the medium and then daily with each change of medium for 4 days, and the effect
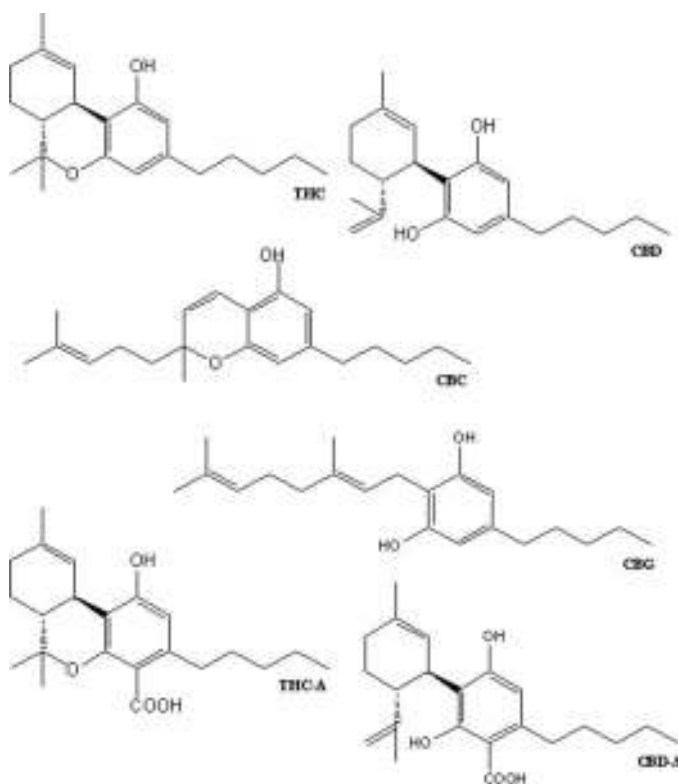

Fig. 1. Chemical structures of the plant-derived cannabinoids used in this study.

of compounds on cell growth was measured by Crystal Violet vital staining. After staining, cells were lysated in 0.01% acetic acid and analyzed by spectrophotometer analysis (PerkinElmer Lambda 12, $\lambda = 595$ nm; PerkinElmer Life and Analytical Sciences, Boston, MA). Optical density values from vehicle-treated cells were considered as 100% of proliferation. Statistical analysis was performed using ANOVA followed by Bonferroni test.

Detection of Reactive Oxygen Species. Intracellular reactive oxygen species (ROS) generation was determined by spectrofluorometric analysis. MDA-MB-231 cells were plated (16×10^3 cells/well) in Porvair PS-White Microplate 96-well (PerkinElmer Life and Analytical Sciences) for 12 h. The day of the experiment, cells were rinsed once with Tyrode's buffer, then loaded (1 h at 37°C in darkness) with 10 μM 2′,7′-dichlorofluorescein diacetate (fluorescent probe; Molecular Probes, Eugene, OR) in the presence of 0.05% Pluronic F-127. Reactive oxygen species (ROS)-induced fluorescence of intracellular 2′,7′-dichlorofluorescein diacetate was measured with a microplate reader (PerkinElmer LS50B, λ_{Ex}, 495 nm; λ_{Em}, 521 nm). Fluorescence detections were carried out after the incubation of 100 μM H_2O_2 and/or increasing concentrations of cannabidiol at room temperature in the darkness for different times (0–30-60–120 min). The fluorescence measured at time 0 was considered as basal ROS production and subtracted from the fluorescence at different times (Δ_1). Data are reported as mean ± S.E. of Δ_2, i.e., fluorescence Δ_1 values at different doses subtracted of the Δ_1 values of cells incubated with vehicle. In some experiments, a buffer containing $MgCl_2$ in amounts equivalent to $CaCl_2$ and 0.1 mM EGTA and cells preloaded for 30 min with BAPTA-AM (40 μM) were used instead.

Reverse Transcription-Polymerase Chain Reaction Analysis. Total RNAs from these cells were extracted using the Trizol reagent according to the manufacturer's recommendations (Invitrogen, Carlsbad, CA). Following extraction, RNA was precipitated using ice-cold isopropanol, resuspended in diethyl pyrocarbonate (Sigma-Aldrich)-treated water, and its integrity was verified following separation by electrophoresis on a 1% agarose gel containing ethidium bromide. RNA was further treated with RNase-free DNase I (Ambion DNA-free kit; Ambion, Austin, TX) according to the manufacturer's recommendations to digest contaminating genomic DNA and to subsequently remove the DNase and divalent cations.

The expression of mRNAs for CB_1, CB_2, TRPV1, and GAPDH were examined by semiquantitative RT-PCR. Total RNA was reverse-transcribed using random primers. DNA amplifications were carried out in PCR buffer (Invitrogen) containing 2 μl of cDNA, 500 μM dNTP, 2 mM MgCl2, 0.8 μM of each primer, and 0.5 U of *Taq* polymerase platinum (Invitrogen). The thermal reaction profile consisted of a denaturation step at 94°C for 1 min, annealing at 55°C (GAPDH) or 57°C (CB_2 and TRPV1) or 60°C (CB_1) for 1 min, and an extension step at 72°C for 1 min. A final extension step of 10 min was carried out at 72°C. The PCR cycles observed to be optimal and in the linear portion of the amplification curve were 24 for GAPDH, 29 for CB_1 and CB_2, and 28 for TRPV1 (data not shown). Reaction was performed in a PE Gene Amp PCR System 9600 (PerkinElmer Life and Analytical Sciences). After reaction, the PCR products were electrophoresed on a 2% agarose gel containing ethidium bromide for UV visualization.

Specific rat and human oligonucleotides were synthesized on the basis of cloned rat and human cDNA sequences of CB_1 (GenBank accession nos. NM_012784.3 and X81120 for rat and human, respectively), CB_2 (GenBank accession nos. NM_0205433 and X74328 for rat and human, respectively), TRPV1 (GenBank accession nos. NM_031982 and NM_080706.2 for rat and human, respectively), and GAPDH (GenBank accession nos. NM_017008.2 and BT006893.1 for rat and human, respectively).

For rat and human CB_1, the primers sequences were 5′-GAT GTC TTT GGG AAG ATG AAC AAG C-3′ (nt 1250–1274 for rat and nt 1187–1211 for human; sense) and 5′-AGA CGT GTC TGT GGA CAC AGA CAT GG-3′ (nt 1558–1534 for rat and nt 1495–1470 for human; antisense). The rat CB_2 sense and antisense primers were 5′-TA(C/T) CC(G/A) CCT (A/T)CC TAC AAA GCT C-3′ (nt 407–428) and 5′-C (A/T)GG CAC CTG CCT GTC CTG GTG-3′ (nt 698–676), respectively. For human CB_2, the primers sequences were 5′-TTT CCC ACT GAT CCC CAA TG-3′ (nt 672–691; sense) and 5′-AGT TGA TGA GGC ACA GCA-3′ (nt 1000–983; antisense). For rat TRPV1, the primers sequences were 5′-GAC ATG CCA CCC AGC AGG-3′ (nt 2491–2508; sense) and 5′-TCA ATT CCC ACA CAC CTC CC-3′ (nt 2752–2733; antisense). The human TRPV1 sense and antisense primers were 5′-TGG ACG AGG TGA ACT GGA C-3′ (nt 2761–2779) and 5′-ACT CTT GAA GAC CTC AGC GTC-3′ (nt 3023–3003), respectively. For rat and human GAPDH, the primers sequences were 5′-CCC TTC ATT GAC CTC AAC TAC ATG GT-3′ (nt 949–974 for rat and nt 106–131 for human; sense) and 5′-GAG GGG CCA TCC ACA GTC TTC TG-3′ (nt 1418–1396 for rat and nt 575–553 for human; antisense).

The expected sizes of the amplicons were 309 bp for rat and human CB_1, 291 bp for rat CB_2, 329 bp for human CB_2, 263 bp for rat TRPV1, 262 bp for human TRPV1, and 470 bp for rat and human GAPDH. In the presence of contaminant genomic DNA, the expected size of the amplicons would be 1062 bp for GAPDH (data not shown). No PCR product was detected when the reverse transcriptase step was omitted.

Western Immunoblotting Analysis for Caspase-3. Immunoblotting analysis was performed on the cytosolic fraction of cells treated as described above and according to previous published work (Iuvone et al., 2004). Cytosolic fraction proteins were mixed with gel loading buffer (50 mM Tris/10% SDS/10% glycerol 2-mercaptoethanol/2 mg of bromphenol/ml) in a ratio of 1:1, boiled for 5 min and centrifuged at 10,000g for 10 min. Protein concentration was determined, and equivalent amounts (50 μg) of each sample were separated under reducing conditions in 12% SDS-polyacrylamide minigel. The proteins were transferred onto nitrocellulose membrane, according to the manufacturer's instructions (Bio-Rad, Hercules, CA). The membranes were blocked by incubation at 4°C overnight in high-salt buffer (50 mM Trizma base, 500 mM NaCl, 0.05% Tween 20) containing 5% bovine serum albumin and then incubated for 2 h with anticaspase 3 (1:2000, v/v) at room temperature, followed by incubation for 2 h with horseradish peroxidase-conjugate secondary antibody (Dako, Glostrup, Denmark). The immune complexes were developed using enhanced chemiluminescence detection reagents (GE Healthcare, Little Chalfont, Buckinghamshire, UK) according to the manufacturer's instructions and exposed to Kodak X-OMAT film (Eastman Kodak, Rochester, NY). The bands of τ protein on X-ray film were scanned and densitometrically analyzed with a GS-700 imaging densitometer.

Immunofluorescence. For immunoreaction, MDA-MB-231 cells were seeded on sterile coverslips (22 × 22 mm; Menzel, Braunschweig, Germany) in six-well culture plates and incubated under standard conditions until they were at least 70% confluent. Cultured cells were processed for immunofluorescence. After three washes with PBS, cells were fixed by incubating them in 4% (v/v) paraformaldehyde in PBS for 20 min at room temperature, rinsed with PBS, permeabilized for 15 min in 0.5% Triton X-100 in PBS, and incubated overnight at 4°C with rabbit polyclonal rabbit anti-CB_1 or anti-CB_2 antibody (Cayman Chemical, Ann Arbor, MI), both diluted 1:50 in 0.5% Triton X-100 in PBS, or goat anti-TRPV1 antibody (Santa Cruz Biochemicals, Santa Cruz, CA) diluted 1:100 in 0.5% Triton X-100 in PBS. After three washes in PBS, fluorescence was revealed by incubation for 2 h in an Alexa Fluor 488-labeled secondary anti-rabbit antibody (Invitrogen) diluted 1:100 in 0.5% Triton X-100 in PBS or Alexa Fluor 546-labeled secondary anti-goat antibody (Invitrogen) diluted 1:200 in 0.5% Triton X-100 in PBS. The preabsorption of antibodies with the respective blocking peptides as well as omission of primary antibodies (control immunoreaction) resulted in much weaker or negative staining, respectively. Sections processed for immunofluorescence were studied with an epifluorescence microscope equipped with the appropriate filter (Leica DM IRB; Leica, Wetzlar, Germany). Images were acquired using a digital Leica DFC

320 camera connected to the microscope and the image analysis software Leica IM500. Images were processed in Adobe Photoshop (Adobe Systems, Mountain View, CA), with brightness and contrast being the only adjustments made.

In Vivo Studies: Effect on Xenograft Models of Carcinoma. All of the experiments were performed by using Charles River 6-week-old male athymic mice (Charles River, Margate, Kent, UK) as described previously (Bifulco et al., 2001). Two different mouse xenograft models of tumor growth were induced by s.c. injection (5×10^5 cells) of two distinct highly invasive tumoral cell lines (KiMol or MBA-MD-231 cells) into the dorsal right side of athymic mice. Starting from the appearance of tumoral mass, pure compounds or *Cannabis* extracts were injected intratumor in the same inoculation region twice per week for 20 (KiMol cell-induced tumors) or 16 (MBA-MD-231 cell-induced tumors) days. THC and cannabidiol were administered at the dose of 5 mg/kg, whereas THC-rich and cannabidiol-rich were administrated at the dose of 6.5 mg/kg, which contains 5 mg/kg THC and cannabidiol, respectively. Tumor diameters were measured with calipers every other day until the animals were killed. Tumor volumes (V) were calculated by the formula of rotational ellipsoid (V = AxB2/2; A = axial diameter, B = rotational diameter). Results were reported as means ± S.E. Statistical analysis was performed using ANOVA followed by the Bonferroni's test.

In Vivo Analysis: Effect on Experimental Lung Metastasis. Monocellular suspension of MDA-MB-231 cells containing 2.5×10^5 cells was injected into the left paw of 30-day-old BalB/c male mice. Animals were divided into three groups: vehicle ($n = 11$), cannabidiol (5 mg/kg/dose, $n = 14$), or cannabidiol-rich (6.5 mg/kg/dose, $n = 14$). The drugs were injected i.p. every 72 h. Experimental metastases were evaluated 21 days after the injection. To contrast lung nodules, lungs were fixed in Bouin's fluid, and metastatic nodes were scored on dissected lung under a stereoscopic microscope. All animal studies were conducted in accordance with the Italian regulation for the welfare of animals in experimental neoplasia. All data were presented as means ± S.D. Statistical analysis was performed using one-way ANOVA.

Cell Cycle and Apoptosis Detection. Different cell lines were exposed to 10 μM of cannabidiol or cannabigerol for 48 h at 37°C in a humidified atmosphere containing 5% CO_2. The distribution of cells among the different phases of the cell cycle and apoptosis rate were evaluated by flow cytometric analysis of the DNA content. Cells (5×10^5) were collected, washed twice with PBS, fixed by ethanol 70%, and kept at -20°C for at least 4 h. Propidium iodide (10 μg/ml) in PBS containing 100 U/ml DNase-free RNase was added to the cells for 15 min at room temperature. Cells were acquired by a FACScalibur flow cytometer (BD Biosciences, San Jose, CA), and then analysis was performed using ModFit LT version 3.0 from Verity Software House, Inc. (Topsham, ME); 10,000 events were collected and corrected for debris and aggregate populations.

Anandamide Cellular Reuptake and Intracellular Hydrolysis. The effect of compounds on anandamide cellular reuptake was analyzed on rat basophilic leukemia cells or MDA-MB-231 cells by using 2.5 μM (10,000 cpm) [14C]anandamide as described previously

(De Petrocellis et al., 2000). Briefly, cells were incubated with [14C]anandamide for 5 min at 37°C, in the presence or absence of varying concentrations of the compounds. Residual [14C]anandamide in the incubation medium after extraction with $CHCl_3/CH_3OH$ 2:1 (by volume), determined by scintillation counting of the lyophilized organic phase, was used as a measure of the anandamide that was taken up by cells (De Petrocellis et al., 2000). Nonspecific binding of [14C]anandamide to cells and plastic dishes was determined in the presence of 100 μM anandamide and was never higher than 30%. Data are expressed as the concentration exerting 50% inhibition of anandamide uptake (IC_{50}) calculated by GraphPad software (GraphPad Software Inc., San Diego, CA). The effect of compounds on the enzymatic hydrolysis of anandamide was studied using membranes prepared from N18TG2 cells, incubated with the test compounds and [14C]anandamide (20,000 cpm; 5 μM) in 50 mM Tris-HCl, pH 9, for 30 min at 37°C. [14C]Ethanolamine produced from [14C]anandamide hydrolysis was measured by scintillation counting of the aqueous phase after extraction of the incubation mixture with 2 volumes of $CHCl_3/CH_3OH$ 1:1 (by volume). Data are expressed as the concentration exerting 50% inhibition of [14C]anandamide hydrolysis (IC_{50}), calculated by GraphPad software.

Activity at Human Recombinant TRPV1. The effect of the substances on $[Ca^{2+}]_i$ was determined by using Fluo-3 (Molecular Probes), a selective intracellular fluorescent probe for Ca^{2+} (De Petrocellis et al., 2000). Human embryonic kidney (HEK) 293 cells stably overexpressing human TRPV1 receptor or MDA-MB-231 cells were transferred into six-well dishes coated with poly-L-lysine (Sigma-Aldrich) 1 day prior to experiments and grown in the culture medium mentioned above. On the day of the experiment, the cells (50–60,000 cells/well) were loaded for 2 h at 25°C with 4 μM Flu-3-methylester (Invitrogen) in dimethyl sulfoxide containing 0.04% Pluronic F-127 (Invitrogen). After loading, cells were washed with Tyrode's solution, pH 7.4, trypsinized, resuspended in Tyrode's solution, and transferred to the cuvette of the fluorescence detector (PerkinElmer LS50B) under continuous stirring. Experiments were carried out by measuring cell fluorescence at 25°C ($\lambda_{EX} = 488$ nm, $\lambda_{EM} = 540$ nm) before and after the addition of the test compounds at various concentrations. Data are expressed as the concentration exerting a half-maximal effect (EC_{50}). The efficacy of the effect was determined by comparing it with the analogous effect observed with 4 μM ionomycin. In some experiments with MDA-MB-231 cells, the effect of cannabidiol was measured also in the absence of extracellular Ca^{2+} (i.e., in a Tyrode's solution containing Mg^{2+} instead of Ca^{2+} and 0.1 mM EGTA) and in cells preloaded with BAPTA-AM (20 μM).

Results

Effect on Cancer Cell Growth: In Vitro Studies. For in vitro studies, the cannabinoids under investigation were screened for their ability to reduce cell proliferation on a collection of tumoral cell lines. Cannabidiol always exhibited the highest potency with IC_{50} values ranging between 6.0 ±

TABLE 1
Effect of cannabinoids and *Cannabis* extracts on cancer cell growth

Various epithelial cell lines of various tumoral origin were treated with different concentrations of drugs, and after 4 days, the cell number was measured with Crystal Violet Vital staining (see *Materials and Methods*). Data are reported as mean ± S.E. of IC_{50} values (micromolar) calculated from three independent experiments. CBG, cannabigerol; CBC, cannabichromene; CBD-A, cannabidiol-acid; THC-A, THC-acid; CBD-rich, cannabidiol-enriched cannabis extract; THC-rich, THC-enriched cannabis extract.

	MCF-7	C_6	DU-145	KiMol	CaCo-2	MDA-MB-231	RBL-2H3	AGS
Δ^9-THC	14.2 ± 2.1	23.0 ± 4.2	>25	23.2 ± 1.5	16.5 ± 0.2	24.3 ± 4.2	15.8 ± 3.7	19.3 ± 1.5
THC-A	9.8 ± 0.4	18.0 ± 5.3	>25	21.0 ± 2.7	21.5 ± 1.4	18.2 ± 5.3	10.0 ± 3.4	>25
CBD	8.2 ± 0.3	8.5 ± 0.8	20.2 ± 1.8	6.0 ± 3.0	7.5 ± 0.5	10.6 ± 1.8	6.3 ± 1.5	7.5 ± 1.3
CBD-A	21.7 ± 3.2	18.0 ± 4.2	>25	12.7 ± 3.0	>25	>25	>25	>25
CBG	9.8 ± 3.4	13.0 ± 2.1	21.3 ± 1.7	8.2 ± 0.7	9.0 ± 1.4	16.2 ± 2.1	9.0 ± 0.7	8.2 ± 0.7
CBC	14.2 ± 1.4	13.0 ± 2.6	>25	7.3 ± 3.0	12.0 ± 2.4	20.4 ± 2.6	15.8 ± 4.2	18.3 ± 3.0
THC-rich	21.0 ± 0.5	18.5 ± 3.3	>25	23.0 ± 2.0	16.0 ± 0.5	25.2 ± 3.3	14.6 ± 3.1	22.0 ± 2.0
CBD-rich	6.0 ± 1.0	4.7 ± 0.6	20 ± 4.6	6.2 ± 2.9	12.3 ± 1.2	14.1 ± 1.6	7.0 ± 0.6	10.0 ± 1.9

3.0 and 10.6 ± 1.8 μM (Table 1). Cannabidiol acid was the least potent compound. Among the other plant cannabinoids, cannabigerol was almost always the second most potent compound, followed by cannabichromene (Table 1). The effect of the two *Cannabis* extracts (enriched in cannabidiol or THC) was next investigated, and in some circumstances, the cannabidiol-rich extract appeared slightly more potent than pure cannabidiol (Table 1). In the case of MCF-7 cells, both compounds exhibited quite similar potency, as indicated by the IC$_{50}$ values of 8.2 ± 0.3 and 6.0 ± 1.0 μM, respectively, for cannabidiol and cannabidiol-rich extract (Fig. 2A), on the contrary, in the case of C$_6$ glioma cells, cannabidiol-rich extract also exhibited significantly higher potency than pure cannabidiol (IC$_{50}$, 4.7 ± 0.6 and 8.5 ± 0.8 μM, respectively, $p < 0.05$, Fig. 2B). Only in the case of human DU-145 prostate carcinoma cells, plant cannabinoids induced a stimulatory effect on cancer growth at the lowest doses tested and an inhibitory effect only at the highest concentration tested (25 μM) (as also found by Sanchez et al., 2003 in another prostate carcinoma cell line). In this case, however, the cannabidiol-rich extract lacked the pro-proliferative effect even at the lowest concentration tested of 2 μM (Fig. 2, C and D).

For a comparison, we also tested cisplatinum on some cell lines and found that this widely used anticancer compound as compared with cannabidiol was only 2.5-, 8.8-, and 3.9-fold more potent in MCF-7, MDA-MB-231, and AGS cells (IC$_{50}$ = 3.2 ± 0.3, 1.2 ± 0.2, and 1.9 ± 0.2 μM, respectively) and 17- and 33.6-fold more potent in C$_6$ and DU-145 cells (IC$_{50}$ = 0.5 ± 0.1 and 0.6 ± 0.2 μM, respectively).

The trypan blue dye exclusion method on the entire range of cells was used to detect cytotoxicity and to assess cell viability. All of the compounds under investigation showed a statistically significant cytotoxic effect starting only from the highest concentration tested (25 μM) (data not shown).

Finally, to investigate the selectivity of cannabidiol effect in tumoral versus nontumoral cells, various concentrations (from 1–100 μM) of cannabidiol on different stabilized nontumor cell lines such as HaCat (human keratinocyte), 3T3-F442A (rat preadipocytes), and RAW 264.7 (mouse monocyte-macrophages) were also tested. Cannabidiol, at a dose similar to its IC$_{50}$ values in the various tumoral cell lines, did not affect the vitality of nontumor cell lines (Fig. 2E). Only at a concentration of 25 μM, which exerts nearly 100% inhibition of cancer cell growth, cannabidiol exhibited a cytotoxic effect in these nontumoral cell lines (Fig. 2E). Lastly, it was examined the selectivity of cannabidiol versus a primary cell line derived from mammary glands (human mammary epithelial cells) since several experiments on the mechanism of action of cannabidiol were performed using a human breast carcinoma cell line (MBA-MD-231 cells). Cannabidiol affected significantly the vitality of this cell line only at a 25 μM concentration (Fig. 2F).

Effect on Cancer Cell Growth: In Vivo Studies. For the in vivo studies, the efficacy of cannabidiol and its enriched extract at reducing tumor size and volume was evaluated. Mice treated with either pure cannabidiol or the cannabidiol-rich extract exhibited significantly smaller tumors in comparison with control mice. A strong and statistically significant antitumor effect was observed with both treatments and with both in vivo xenograft tumor models used (Fig. 3, A and B). The effect of cannabidiol and cannabidiol-rich compounds on the formation of lung metastatic nodules of MBA-MD-231 cells injected into the paw was also investigated. Both cannabidiol and cannabidiol-rich exhibited a strong and significant reduction of metastatic lung infiltration (Fig. 3C).

Study on the Cellular Mechanism of Action of Cannabidiol. With the intention to evaluate if the inhibitory effect on cell growth of cannabidiol was associated with apoptotic events or blockade of mitogenesis, the percentage of G$_1$ population cells was estimated by flow cytometry. In MCF-7 cells, a hormone-sensitive cell line, cannabidiol, exerted antiproliferative effect by causing a cell cycle block at the G$_1$/S phase transition (Fig. 4A; Table 2). A similar result was observed in another hormone-sensitive cell line KiMol cells, where, however, the antiproliferative effect of cannabidiol was also accompanied by a proapoptotic action (Fig. 4C; Table 2). Finally, in C$_6$ glioma and MDA-MB-231 cells (two nonhormone-sensitive cell lines), cannabidiol provoked a pure proapoptotic effect (Fig. 4D; Table 2). The proapoptotic effect of cannabidiol on MDA-MB-231 cells was also established by evaluating the involvement of caspase-3. The proapoptotic effect of cannabidiol was confirmed in this cell line but not in DU-145 cells, as indicated by the procaspase-3 cleavage into caspase-3 by Western immunoblotting analysis following a 48-h treatment of cells with the compound (Fig. 4E). In agreement with a role of apoptosis and caspase-3 in cannabidiol anticancer effect in MDA-MB-231 cells, *N*-Acetyl-Asp-Glu-Val-Asp-aldehyde (10 μM), an inhibitor of caspase-3, significantly attenuated the growth-inhibitory effect of both 5 and 10 μM cannabidiol as indicated by the reduction of the percentage inhibition of cell proliferation induced by these two doses of the cannabinoid (from 21.8 ± 3.1 to 7.8 ± 1.1% at 5 μM and from 55.8 ± 4.9 to 11.9 ± 1.6% at 10 μM; means ± S.E.; $n = 3$, $p < 0.01$).

Study on the Molecular Mechanism of Action of CBD. When using PCR, we found that both vanilloid TRPV1 receptors and cannabinoid CB$_1$ and CB$_2$ receptors are expressed in most of the cell lines used in this study (Table 3). To estimate the involvement of TRPV1 receptors in the antiproliferative properties, all cannabinoids were screened for their capability to generate TRPV1-mediated intracellular calcium elevation in stably transfected TRPV1-HEK293 cells. Apart from cannabidiol, only cannabigerol and cannabidiol acid activated TRPV1 receptors, with a significantly lower potency than cannabidiol, whereas cannabichromene, THC, and THC acid were almost inactive (Fig. 5). The cannabidiol-rich extract was as efficacious and potent as cannabidiol, whereas the THC-rich extract was more efficacious and potent than THC, possibly due to the presence of other TRPV1-active cannabinoids, including cannabidiol and cannabigerol (Fig. 5).

To assess whether plant cannabinoids, which are very weak agonists of CB$_1$ and CB$_2$ receptors, activate these receptors indirectly, i.e., by elevating endocannabinoid levels, we studied their effects on anandamide cellular uptake and enzymatic hydrolysis (Bifulco et al., 2004). Although most of the compounds tested did inhibit anandamide metabolism (Table 4), particularly at the level of cellular uptake, their rank of potency (cannabichromene = cannabigerol > cannabidiol = THC) did not reflect their potency at inhibiting cancer cell proliferation.

To conclusively investigate the role of vanilloid TRPV1 receptors and cannabinoid CB$_1$ and CB$_2$ receptors in the
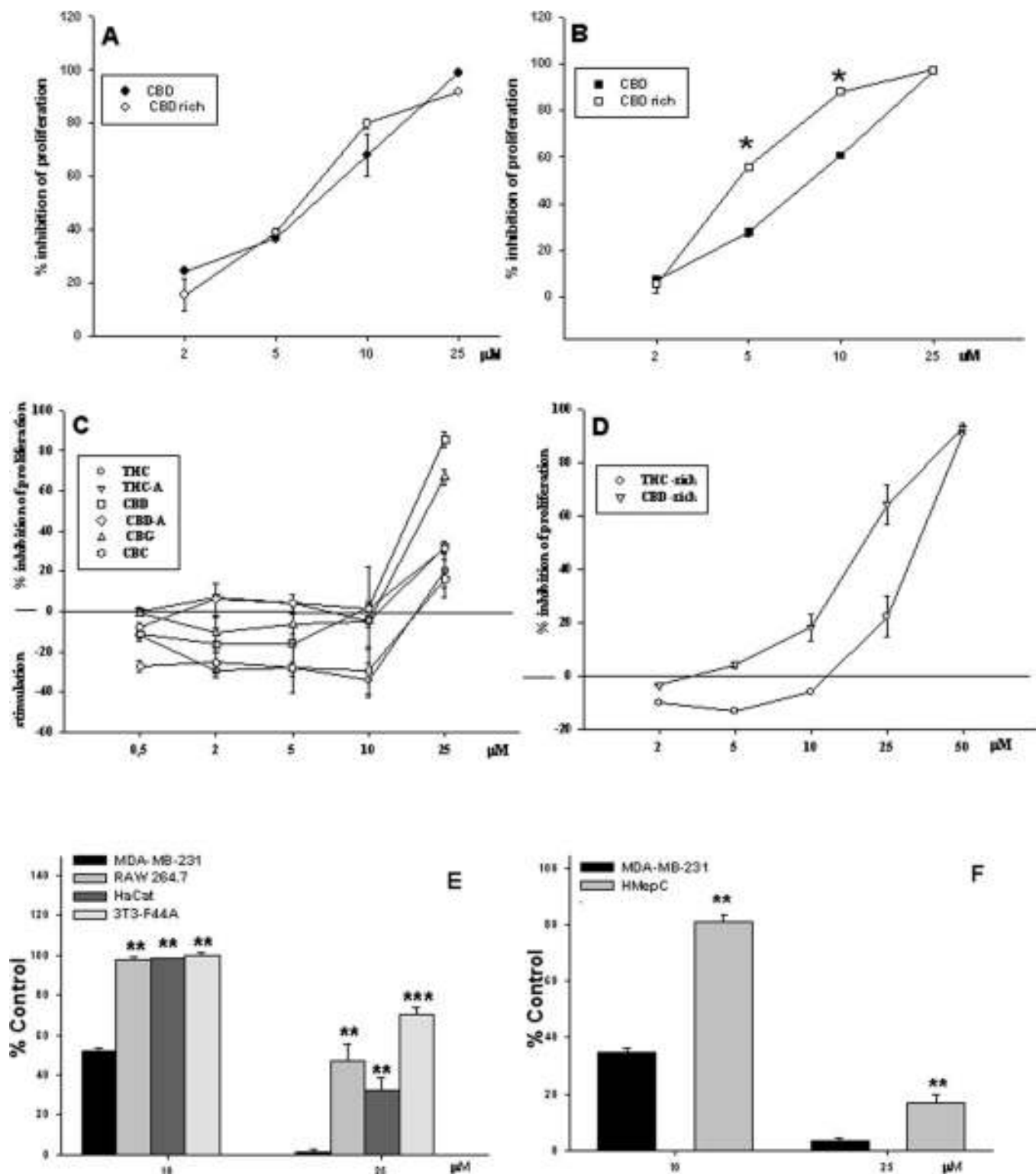
Fig. 2. Effect of cannabinoids and *Cannabis* extracts on the proliferation of some of the cell lines investigated in this study. MCF-7 cells (A), C_6 cells (B), and DU-145 cells (C and D) were treated with increasing concentrations of cannabidiol, cannabinoids (C), and cannabidiol-rich extracts (daily added with each change of medium for 4 days). Effect on cell proliferation was measured by Crystal Violet vital staining. After staining, cells were lysed in 0.01% acetic acid and analyzed by spectrophotometric analysis (PerkinElmer Lambda 12, $\lambda = 595$ nm). Results are reported as percentage of inhibition of proliferation where optical density value from vehicle-treated cells was considered as 100% of proliferation and represent the mean ± S.E. of three different experiments. *, $p < 0.05$ versus cannabidiol pure by ANOVA followed by Bonferroni's test. E and F, effect of cannabidiol on nontumoral cell lines. Cells were treated with two different concentrations of cannabidiol for 4 (E) or 3 days (F), and vitality was evaluated by using trypan blue dye exclusion assay (see *Materials and Methods*). In cells treated with vehicle, mortality was always lower than 2%. Data are expressed as percentage of control and represent the mean ± S.E. of three different experiments. Statistical analysis was carried out by ANOVA followed by Bonferroni's test (**, $p < 0.01$; ***, $p < 0.001$ versus the same concentration of cannabidiol on MDA-MB-231 cells). CBG, cannabigerol; CBC, cannabichromene; CBD-A, cannabidiol acid; THC-A, THC acid; CBD-rich, cannabidiol-enriched cannabis extract; THC-rich, THC-enriched cannabis extract.
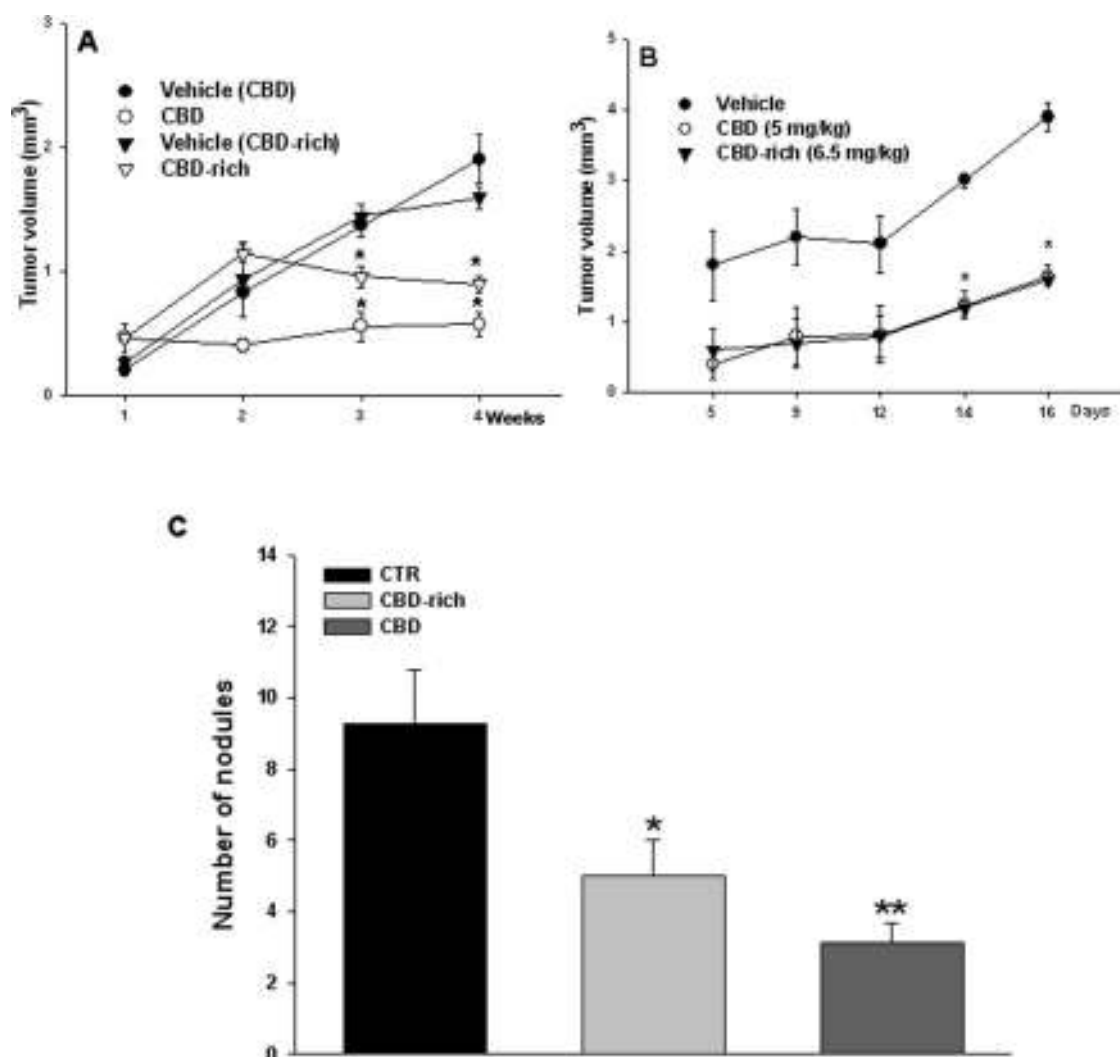
Fig. 3. In vivo actions of cannabidiol on tumor growth and metastasis. A and B, effect of cannabidiol (5 mg/kg) and cannabidiol-rich extract (6.5 mg/kg) on two different xenograft tumor models in athymic mice. KiMol cells (A) or MBA-MD-231 cells (B) were injected s.c. (day 0 of treatment) into the dorsal right side of athymic mice, and the intratumor treatments were administered twice per week. Results represent mean ± S.E. (∗, $p < 0.05$ versus vehicle; $n = 6$ by ANOVA followed by Bonferroni's test). C, effect of cannabidiol and cannabidiol-rich extract on breast cancer cell metastasis. MDA-MB-231 cells were injected into the left paw of 30-day-old BalB/c male mice. Animals were divided into three groups ($n = 11$ for vehicle; $n = 14$ for treated) and treated with vehicle (CTR), cannabidiol (5 mg/kg/dose), or cannabidiol-rich extract (6.5 mg/kg/dose). The drugs were injected i.p. every 72 h. Lung metastatic nodules were evaluated 21 days after the injection. Data represent mean ± S.E. of number of nodules (∗, $p < 0.05$; ∗∗, $p < 0.01$ versus CTR). Statistical analysis was performed by ANOVA followed by Bonferroni's test. CBD-rich, cannabidiol-enriched cannabis extract.

anticancer effects of plant cannabinoids, in all those cell lines where cannabinoid or vanilloid receptors were expressed (Table 3), we studied the effect of selective antagonists, alone or in combination, on the inhibitory effect of 10 μM cannabidiol. Whereas 5′-iodo-resiniferatoxin (I-RTX, 100 nM) was used as a TRPV1-selective antagonist, SR141716A (0.5 μM) and SR144528 (0.5 μM) were used as selective antagonists for CB_1 and CB_2 receptors, respectively. A statistically significant effect of selective concentrations of the two antagonists, I-RTX and SR144528, was found only in MDA-MB-231 cells; however, these molecules were able to revert only partially the effect of cannabidiol. Higher doses of the two compounds inhibited cell number per se and were not used. When I-RTX and SR144528 were administered together, cannabidiol effect was attenuated by about 40%, although this effect was probably minimized by the fact that the mixture of antagonists significantly inhibited cell growth per se (Fig. 6). These findings are in agreement with the results obtained by im-

munofluorescence and showing high levels of CB_2 and TRPV1 receptors in the plasma membrane of intact MDA-MB-231 cells (Fig. 7). Regarding the CB_1 antagonist, despite the presence in MDA-MB-231 cells of CB_1 receptors (Fig. 7), SR141716A (0.5 μM) did not influence the effect of cannabidiol (data not shown). No effect was observed with any of the three antagonists in the other cell lines, except for KiMol cells, were the mixture of antagonists showed a slight inhibition (15 ± 2%), which was not statistically significant (data not shown).

Role of Vanilloid and Cannabinoid Receptors in MDA-MB-231 Cells. Starting from the experiments with TRPV1 and CB_1 and CB_2 receptor antagonists, we further investigated the role of direct or indirect activation of these receptors in cannabidiol effect on MDA-MB-231 cell growth. Cannabidiol and THC-A, tested at a 25 μM concentration, did inhibit the uptake of [^{14}C]anandamide by MDA-MB-231 cells (25.1 ± 2.5% and 21.0 ± 3.0% inhibition, respectively,
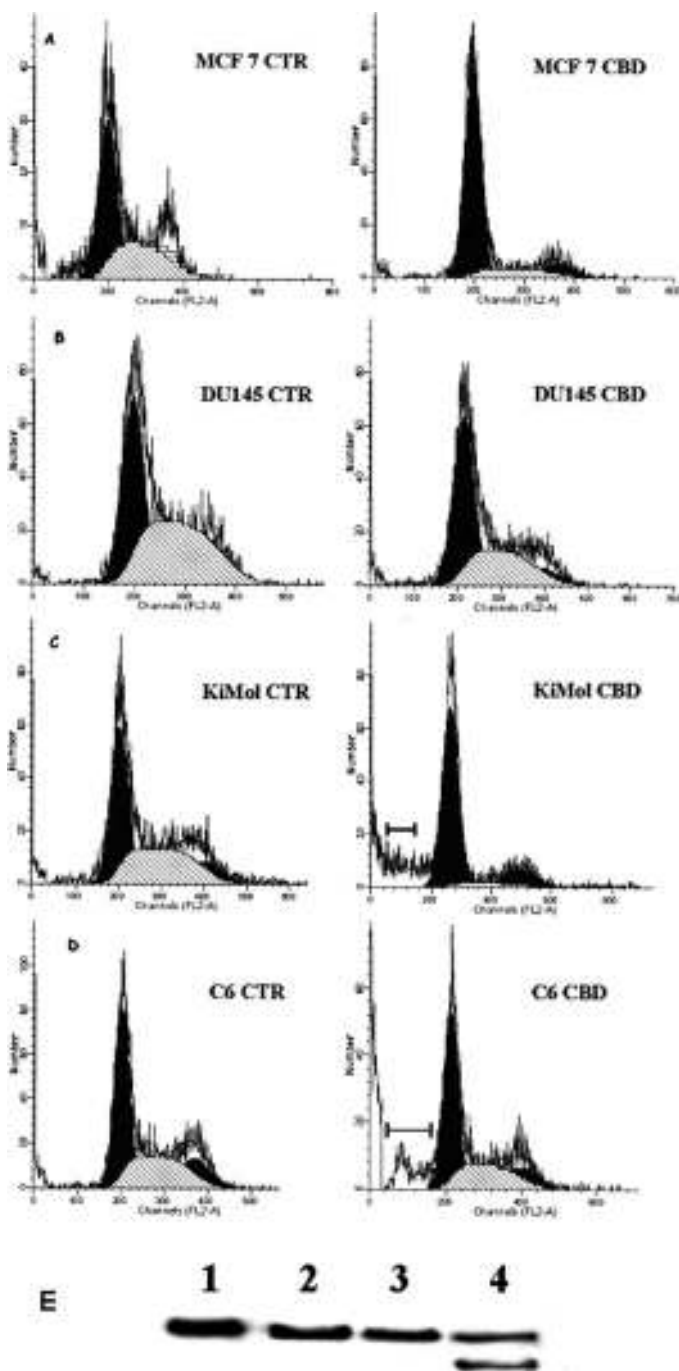
Fig. 4. A to D, representative fluorescence-activated cell sorter analyses showing the effect of 2 days of treatment of 10 μM cannabidiol (CBD) on apoptosis rate in various cell lines calculated as the percentage of cells showing a subdiploid DNA peak (subG1). Graphs are representative of three independent experiments with similar results. Graphs on the left are from cells treated with vehicle and those on the right from cells treated with cannabidiol. Line bar shows where the subdiploid DNA peak is calculated. CTR, vehicle-treated cells. E, effect of cannabidiol on caspase 3 release from procaspase. Western immunoblotting analysis was performed to detect the levels of caspase-3 expression. Proteins were extracted from DU-145 cells (lanes 1 and 2) or MDA-MB-231 cells (lanes 3 and 4) treated with vehicle (CTR, lanes 1 and 3) or 10 μM cannabidiol (cannabidiol, lanes 2 and 4) for 48 h. Determination of relative band intensity was carried out using a GS700 densitometer, and the results are presented in arbitrary scanning units. DU-145, CTR = 5.7 $\pm$ 0.81; cannabidiol = 4.2 $\pm$ 0.74; MDA-MB-231, CTR = 3.11 $\pm$ 0.67; cannabidiol = 2.64 $\pm$ 0.26 (Procaspase), 2.89 $\pm$ 0.51 (Caspase), mean $\pm$ S.E. of $n = 3$ separate experiments.

TABLE 2

Determination of cell cycle arrest, apoptosis, and mortality in the various cell lines exposed for 48 h to 10 μM of cannabidiol before flow cytometry analysis (see Fig. 4 and *Materials and Methods*); each experiment was repeated three times

Cell Type	Cell Cycle Arrest	Apoptosis	Mortality
DU-145	Absent	<10	Absent
MCF-7	G_1/S	Absent	Absent
C_6	Absent	9–10%	25–27%
KiMol	G_1/S	12–15%	20–22%
MDA-MB-231	Absent	15%	Absent

TABLE 3

Schematic and qualitative representation of the results of the RT-PCR analyses of mRNAs for cannabinoid and vanilloid receptors in the cell lines under study

Total RNA from cells was extracted, and its integrity was verified. RNA was further treated with RNase-free DNase I (Ambion DNA-free kit) to digest contaminating genomic DNA and to subsequently remove the DNase and divalent cations. The expression of mRNAs was examined by RT-PCR. Transcripts for fatty acid amide hydrolase (FAAH) and CB_1 and CB_2 receptors were analyzed and are classified as: a, abundant; m, medium; w, weak; and nd, not detected, based on the intensity of the band normalized to the band corresponding to glyceraldehyde-3-phosphate dehydrogenase as the housekeeping gene and on the number of cycles necessary to obtain a visible band. Results are based on $n = 3$ separate determinations.

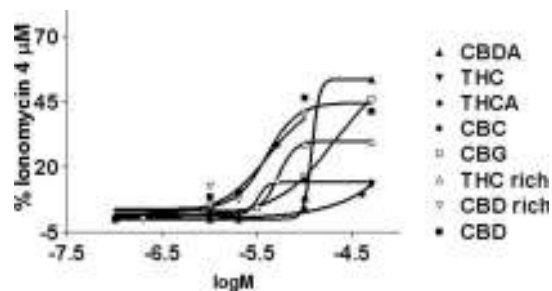| Cell Type	CB_1	CB_2	TRPV1
AGS	nd	nd	a
DU-145	a	w	a
MCF-7	w	w	a
C_6	m	w	m
KiMol	w	a	m
CaCo-2	w	a	a
RBL-2H3	nd	a	nd
MDA-MB-231	w	m	a

Fig. 5. Effect of plant cannabinoids and *Cannabis* extracts on vanilloid TRPV1 receptor activation. HEK293 cells overexpressing the human recombinant TRPV1 receptor were loaded with a selective fluorescent probe (see *Materials and Methods*). The TRPV1-mediated effect on $[Ca^{2+}]_i$ was determined by measuring cell fluorescence before and after the addition of the test compounds at increasing concentrations. Data are reported as percentage of the maximal effect obtained with Ionomycin 4 μM and are means of $n = 3$ separate experiments. Error bars are not shown for the sake of clarity and were never higher than 5% of the means. CBG, cannabigerol; CBC, cannabichromene; CBD-A, cannabidiol-acid; THC-A, THC acid; CBD-rich, cannabidiol-enriched cannabis extract; THC-rich, THC-enriched cannabis extract.

mean $\pm$ S.E.; $n = 4$), but cannabigerol and a selective inhibitor of anandamide cellular uptake, (*S*)-1′-(4-hydroxybenzyl)-*N*-ethyl-oleoylamide, were significantly more efficacious at exerting this effect (82.0 $\pm$ 3.5% and 77.0 $\pm$ 3.1% inhibition, respectively), even though they were significantly less efficacious than cannabidiol at inhibiting cell growth (Table 1; data not shown). Furthermore, direct agonists of CB_1 and CB_2 receptors, i.e., arachidonoylchloroethanolamide and JWH-133, were also less potent and efficacious than cannabidiol at inhibiting MDA-MB-231 cell growth (data not shown). We also studied in MDA-MB-231 cells the effect of

TABLE 4

Effect of plant cannabinoids on anandamide inactivation

Membranes from N18TG2 cells were incubated with [^{14}C]anandamide in the presence of compounds for 30 min at 37°C (see *Material and Methods*) to determine the effect on the enzymatic hydrolysis by fatty acid amide hydrolase (FAAH). Intact RBL-2H3 cells were incubated with [^{14}C]anandamide in the presence of compounds for 5 min at 37°C (see *Material and Methods*) to determine the effect on anandamide cellular uptake (ACU). Data represent mean ± S.E. of three different experiments.

	FAAH Assay IC$_{50}$	ACU Assay IC$_{50}$
	μM	
THC	>50	22 ± 5
CBD	28 ± 3[a]	22 ± 2[a]
CBG	>50	15 ± 3
CBC	>50	13 ± 2
THC-A	>50	>25
CBD-A	>50	>25

CBG, cannabigerol; CBC, cannabichromene; CBD-A, cannabidiol-acid; THC-A, THC-acid.
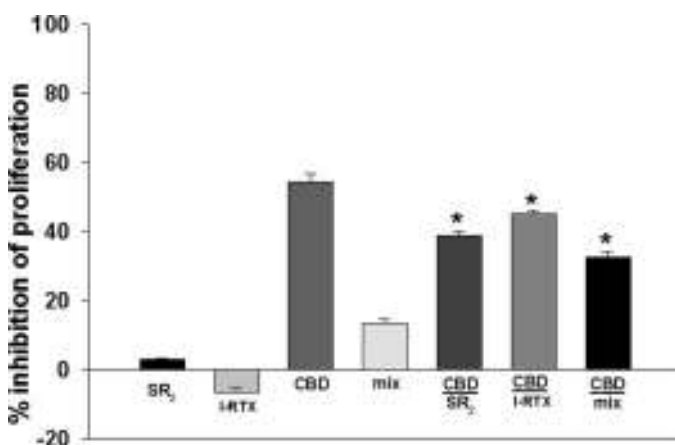
[a] Data from Bisogno et al., 2001.

Fig. 6. Influence of selective receptor antagonists on CBD antiproliferative action. MDA-MB-231 cells were treated with 10 μM cannabidiol in presence or in absence of selective antagonist for CB$_2$ receptors [0.5 μM SR144528 (SR$_2$)], TRPV1 receptors [100 nM 5′-I-resiniferatoxin (I-RTX)], or a mixture of both compounds (mix). Data are shown as percent inhibition of proliferation. Cells vehicle-treated were used as 100% of proliferation. *, $p < 0.05$ versus cannabidiol only, by ANOVA followed by Bonferroni's test.

cannabidiol (5 μM) after a 10-min exposure to methyl-β-cyclodextrin (0.5 mM), a potent membrane cholesterol depleter that is able to destroy the lipid raft microdomains and to block the clustering of CB$_1$ at the plasma membrane in MDA-MB-231 cells (Sarnataro et al., 2005). We found no significant
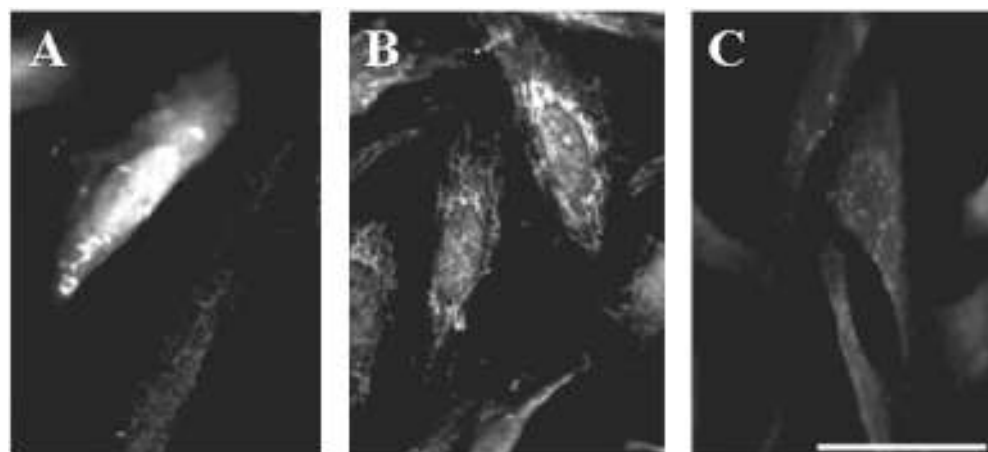
effect on the inhibitory action of cannabidiol (from 29.9 ± 3.5% to 30.2 ± 3.6% inhibition, mean ± S.E.; $n = 3$; $p > 0.05$).

Regarding TRPV1 receptors, we investigated whether cannabidiol induces intracellular Ca^{2+} elevation also in MDA-MB-231 cells. Cannabidiol did induce a rapid and sustained elevation of intracellular Ca^{2+} in MDA-MB-231 cells (EC$_{50}$ = 0.7 ± 0.1 μM, maximal effect at 10 μM cannabidiol = 24.5 ± 0.3% of the effect of 4 μM ionomycin, Fig. 8, A and B) but in a way that was not blocked by I-RTX, nor by CB$_1$ or CB$_2$ receptor antagonists (Fig. 8D). In agreement with these data, we also found that potent selective agonists of TRPV1 receptors, such as capsaicin and RTX, respectively, exerted little effect on MDA-MB-231 cell growth (data not shown). Moreover, cannabidiol effect on intracellular Ca^{2+} did not require the presence of extracellular Ca^{2+} (EC$_{50}$ = 0.14 ± 0.01 μM, Fig. 8C), indicating that it occurs mostly at the level of intracellular stores and was in fact blocked after loading the cells with the Ca^{2+} chelating agent BAPTA-M (Fig. 8D).

Involvement of Oxidative Stress in CBD Actions on MDA-MB-231 Cells. MDA-MB-231 cells were selected also to investigate the implications of cannabidiol effects on oxidative stress phenomena. The effects of antioxidant agents on the antiproliferative action of 10 μM cannabidiol were evaluated. Already at 0.1 μM concentration, α-tocopherol significantly prevented, although in a partial manner, the antiproliferative effects of cannabidiol on these cells (Fig. 9A); also, vitamin C and astaxantine, at 25 μM concentration, were able to counteract the inhibitory effect of cannabidiol by ~30% (data not shown). Further experiments were performed to measure the intracellular ROS generation. Cannabidiol in a dose- and time-dependent manner induced ROS formation in MDA-MB-231 cells in a Ca^{2+}-containing buffer (Fig. 9B). Importantly, the effect of cannabidiol (10 μM) on ROS production (60 min) was Ca^{2+}-dependent because it was erased when cells were preloaded with BAPTA-AM (40 μM) and incubated in an isotonic buffer with the same ionic strength but with Mg^{2+} instead of Ca^{2+} (Fig. 9B, inset). Next, we carried out different incubations under both standard and severe growth cell culturing conditions that lead to a strong production of ROS, i.e., with 12-h serum deprivation; subsequently, cells were treated either with low or high concentration of cannabidiol only for 24 h, as opposed to the 96-h incubation used in most of the experiments presented here. In nonserum-deprived cells, cannabidiol exerted
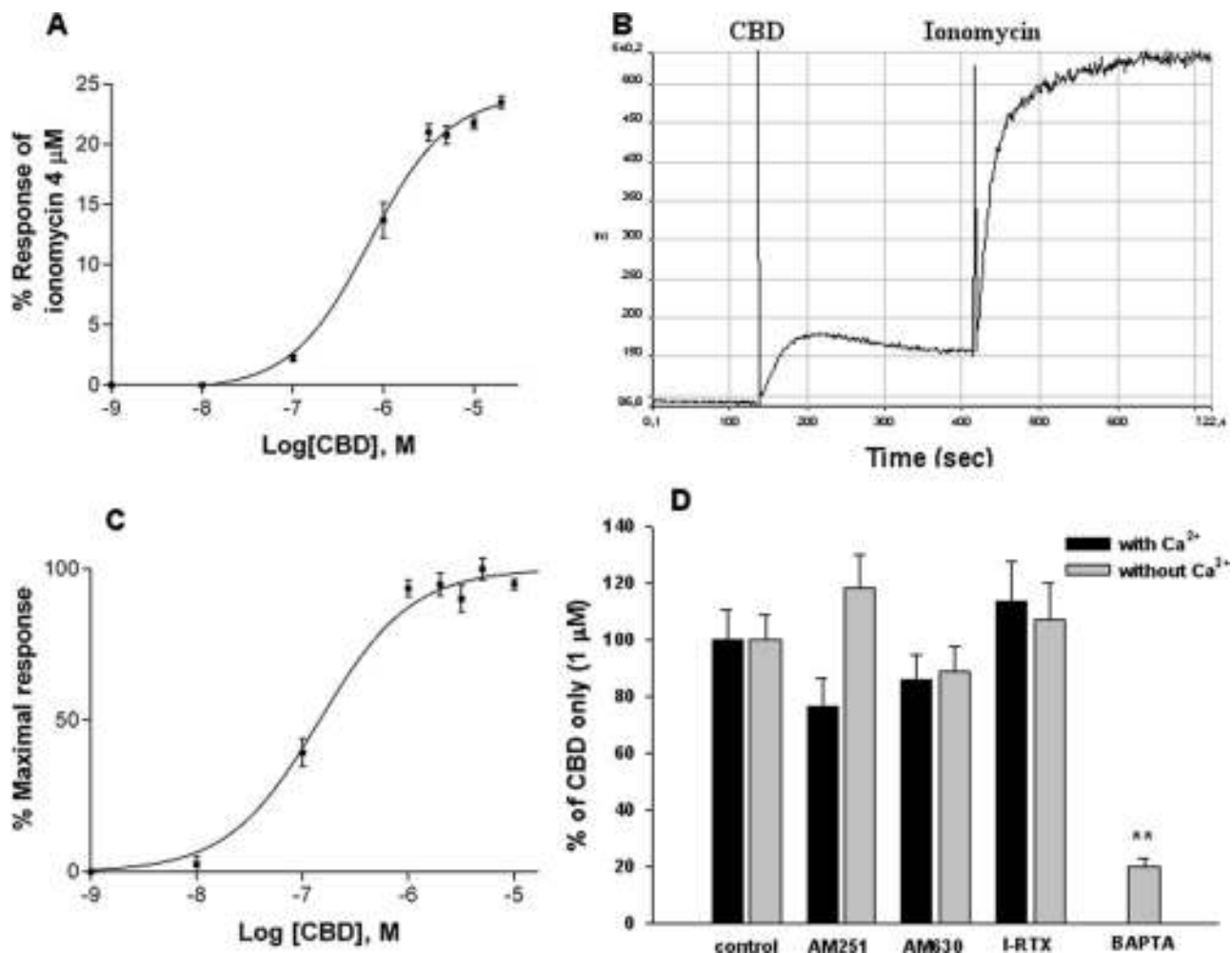
Fig. 7. Representative photomicrographs demonstrating localization of CB$_1$, CB$_2$, and TRPV1 receptors in human breast adenocarcinoma (MDA-MB-231) cells as determined by the immunofluorescence technique described under *Materials and Methods*. A, CB$_1$ receptor immunoreactivity. B, CB$_2$ receptor immunoreactivity. C, TRPV1-immunoreactivity was performed using rabbit polyclonal anti-CB$_1$, anti-CB$_2$ (both diluted 1:50), and Alexa Fluor 488-conjugated secondary antibody (1:100) and goat polyclonal anti-TRPV1 diluted 1:100 and Alexa Fluor 546-conjugated secondary antibody (1:200). Magnification, 63×. Scale bar, 40 μm. Immunofluorescence was almost undetectable when preincubating antibodies with the corresponding blocking peptides (data not shown).

Fig. 8. Effect of CBD on intracellular Ca^{2+} in MDA-MB-231 cells. A, dose-related effect of cannabidiol in the presence of extracellular Ca^{2+}, as determined with Fluo-4. Data are mean $\pm$ S.E. of $n = 4$ experiments and are expressed as percentage of the effect obtained with 4 μM ionomycin. B, time-related effect of cannabidiol (10 μM) in the presence of extracellular Ca^{2+}. Trace is representative of $n = 4$ experiments. C, dose-related effect of cannabidiol in the absence of extracellular Ca^{2+}, as determined with Fura-2. Data are mean $\pm$ S.E. of $n = 4$ experiments. Maximal $\Delta_{fluorescence}$ was 0.235 $\pm$ 0.031 at 10 μM cannabidiol and was usually attained after 200 s (D). Effect of various antagonists (the CB_1 antagonist AM251, 1 μM; the CB_2 antagonist AM630, 1 μM; the TRPV1 antagonist I-RTX, 0.1 μM; 5-min pretreatment) and the intracellular calcium chelating agent BAPTA-AM (20 μM, loaded onto the cells before stimulation) on cannabidiol (1 μM) action on intracellular Ca^{2+}. Similar results were obtained with SR141716A and SR144528.

a pro-proliferative effect at low doses (0.5 μM), whereas it was ineffective after serum deprivation (Fig. 9, A and B). At the highest concentration tested (10 μM), the growth-inhibitory effect was much stronger than that caused by the same dose without serum deprivation (Fig. 10, A and B). The effect of cannabidiol on ROS formation induced by 100 μM H_2O_2 was also measured. In conformity with the results obtained in the short-term cell proliferation assays, cannabidiol, despite its stimulatory activity on ROS formation when administered per se (Fig. 9B), was able to reduce ROS production induced by 100 μM H_2O_2, but only at the lowest concentration tested (Fig. 10C).

Discussion

The aim of this study was to identify natural cannabinoids with antitumor activities at least similar to those of THC and devoid of the potential central effects of this compound. Given that the efficacy of cannabinoids as antitumoral agents appears to be strictly correlated to the cell type under investigation, we screened a panel of plant cannabinoids in a wide

range of tumoral cell lines distinct in origin and typology. We found that, surprisingly, cannabidiol acted as a more potent inhibitor of cancer cell growth than THC and that cannabigerol and cannabichromene usually followed cannabidiol in the rank of potency. The cell growth-inhibitory effect of cannabidiol depended on its chemical structure since the addition of a carboxylic acid group (as in cannabidiol acid) dramatically reduced its activity. This is unlikely due to simple modification of the lipophilicity of the compound and subsequent decrease of its capability to penetrate the cell membrane since THC-A was often more efficacious than THC. We also found that the cannabidiol-rich *Cannabis* extract was as potent as pure cannabidiol in most cases or even more potent in some cell lines. These results suggest the use in cancer therapy for cannabidiol, a compound lacking the psychotropic effects typical of THC. Indeed, the efficacy of cannabidiol and of the cannabidiol-rich extract were confirmed in vivo in two different models of xenograft tumors obtained by inoculation in athymic mice of either v-K-*ras*-transformed thyroid epithelial cells or of the highly invasive MDA-MB-231 breast
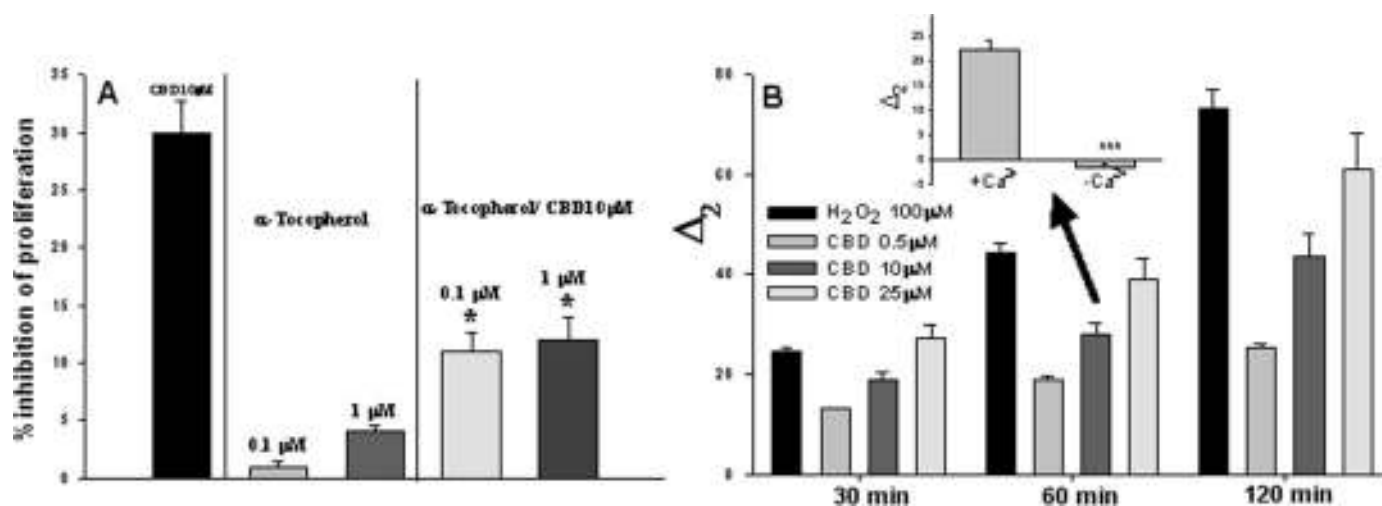
Fig. 9. Study of the involvement of oxidative stress in the effect of CBD. A, antiproliferative effect of 10 μM cannabidiol on MDA-MB-231 cells was measured after 4 days of treatment in absence or in presence of increasing concentrations of α-tocopherol. Data represent mean $\pm$ S.E. of percent inhibition of proliferation (*, $p < 0.05$ by ANOVA followed by Bonferroni's test). B, time course of ROS production by MDA-MB-231 cells (16 $\times$ 10^3 cells/well) as measured by spectrofluorometric analysis. Cells were loaded 1 h with 10 μM fluorescent probe in the presence of 0.05% Pluronic; fluorescence was measured in a 96-well microplate reader (PerkinElmer LS50B, λ_{Ex}, 495 nm; λ_{Em}, 521 nm). Fluorescence detection was carried out after the incubation of either 100 μM H$_2$O$_2$ or increasing concentrations of cannabidiol at different times (0–30-60–120 min). 100 μM H$_2$O$_2$ was used as a positive control in these experiments. The fluorescence measured at time 0 was considered as basal ROS production and subtracted from the fluorescence at different times (Δ_1). Data are reported as Δ_2, i.e., Δ_1 values at different doses subtracted of the Δ_1 values of cells incubated with vehicle, and are mean $\pm$ S.E. of $n = 3$ experiments. The effects of H$_2$O$_2$ and of all doses of cannabidiol were significantly different from control values as determined by ANOVA followed by Bonferroni's test. Inset, lack of effect of cannabidiol 10 μM on ROS production (after 60 min) in the absence of both extracellular and intracellular Ca^{2+} is shown. ***, $p < 0.005$ by ANOVA, $n = 5$.
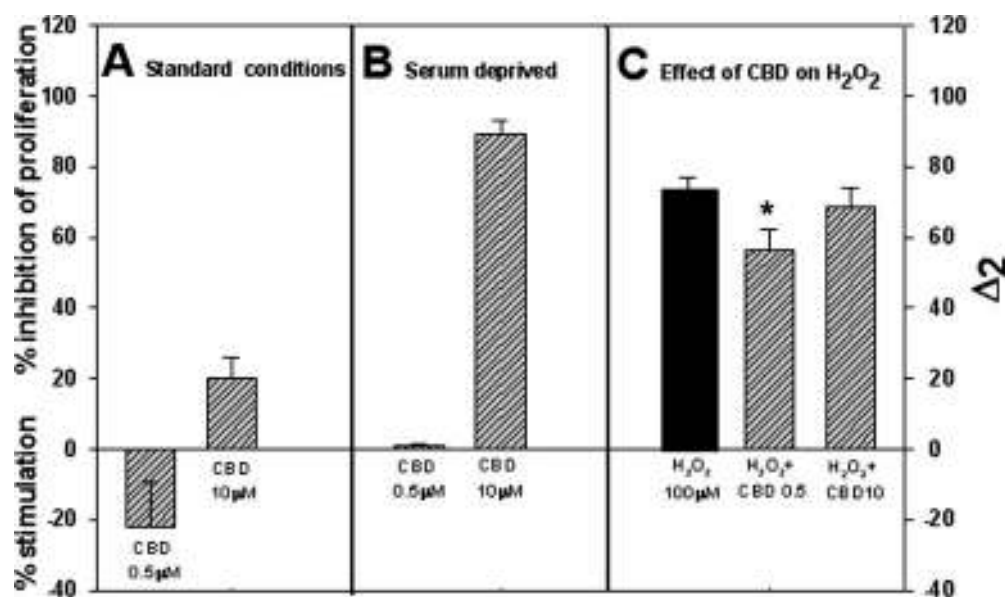

Fig. 10. Study of the involvement of oxidative stress in the effect of CBD. A and B, antiproliferative effect of cannabidiol (24-h incubation) was evaluated in standard growth conditions or after 12 h of serum deprivation to induce oxidative stress. Poststarvation, cells were treated with 0.5 or 10 μM cannabidiol for 24 h, and the effect on proliferation was evaluated by Crystal Violet staining. Data are reported as mean $\pm$ S.E. of percent inhibition of proliferation, $n = 3$. C, ROS production after 2 h of incubations with cannabidiol or H$_2$O$_2$ was measured in MDA-MB-231 cells (16 $\times$ 10^3 cells/well) by spectrofluorometric analysis. The effect of cannabidiol per se (0.5 and 10 μM) is reported in Fig. 9. Cells were loaded 1 h with 10 μM fluorescent probe in presence of 0.05% Pluronic, and fluorescence was measured in a 96-well microplate reader (PerkinElmer LS50B, λ_{Ex}, 495 nm; λ_{Em}, 521 nm). Fluorescence was measured at $t = 0$ and after 2 h of incubation with H$_2$O$_2$ in the presence or absence of increasing concentration of cannabidiol. Data are expressed as explained in the legend to Fig. 9. Cannabidiol inhibited ROS production by H$_2$O$_2$ only at the lowest concentration (0.5 μM, $p < 0.05$ by ANOVA followed by Bonferroni's test).

cancer cells. Furthermore, cannabidiol and the cannabidiol-rich extract also inhibited the formation of lung metastases subsequent to inoculation of MDA-MB-231 cells, in agreement with the inhibitory actions on cancer cell migration previously described for this compound (Vaccani et al., 2005).

The weak effects observed here with THC might be regarded as surprising. In fact, THC was reported to induce

apoptosis in both C$_6$ glioma and human prostate PC-3 cells (Sanchez et al., 1998; Ruiz et al., 1999; Sarfaraz et al., 2005), although it may even enhance breast cancer growth and metastasis (McKallip et al., 2005). The low potency found here for this compound, at least in glioma and prostate cancer, could be explained by the different experimental conditions used and supports the notion that the efficacy of can-

nabinoids is strongly dependent on the cell type utilized. In fact, regarding glioma cells, THC induction of apoptosis was reported not in C_6 cells, but in a THC-sensitive subclone ($C_{6.9}$). Furthermore, Ruiz et al. (1999) used a human prostate cancer cell line different from the one used here. Melck et al. (2000) found that stimulation of CB_1 receptors causes inhibition of DU-145 cell proliferation only when this is induced by nerve growth factor. Using similar culturing conditions as those used here, we previously showed that CB_1, but not CB_2, stimulation inhibits the proliferation of MCF-7, KiMol, and CaCo-2 cells more potently than what observed here with THC (De Petrocellis et al., 1998; Bifulco et al., 2001; Ligresti et al., 2003). This might be due to the use in those studies of CB_1 agonists with higher potency or efficacy than THC or of cells clones with a higher expression of CB_1 receptors than that observed here. Indeed, McKallip et al. (2005) proposed for human breast cancer cells that resistance to THC toxicity is correlated to low expression of CB_1 receptors and high expression of vanilloid receptors.

To date, the receptor-mediated anticancer effects of cannabinoids and endocannabinoids have been ascribed to either CB_1-mediated inhibition of mitosis, as in the case of some hormone-sensitive cells, or to the induction of apoptosis following activation of TRPV1 and/or CB_2 receptors. Starting from the hypothesis that cannabidiol decreased cell number by induction of apoptosis at least for human glioma cell lines (Massi et al., 2004), we decided to evaluate the percentage of apoptotic cells after exposure to cannabidiol and found that the effect of the compound was due to an arrest of the cell cycle in the case of MCF-7 (hormone-sensitive) cells, to both cell cycle arrest and apoptosis in KiMol cells (which are also hormone-sensitive to some extent), and only to induction of apoptosis in C_6 and MDA-MB-231 (nonhormone-sensitive) cells. It was, therefore, clear that cannabidiol lacks a unique mode of action for its anticancer effect on the cell lines under investigation. Based on previous evidence that cannabidiol, although inactive as a direct agonist at cannabinoid CB_1 and CB_2 receptors, activates directly the vanilloid TRPV1 receptor and is capable of increasing endocannabinoid levels by inhibiting their inactivation (Bisogno et al., 2001), we first investigated the capability of plant cannabinoids to interact with the key components of the endocannabinoid or endovanilloid systems. Indeed, cannabidiol, cannabigerol, and cannabichromene were found here to activate TRPV1 receptors and/or inhibit anandamide inactivation to some extent. However, despite the presence of either cannabinoid or vanilloid receptors (or both) in all cell lines under study, in none but one of these cell lines the direct or indirect stimulation of these receptors seemed to be entirely or even partially responsible for the anticancer effects of cannabidiol. The only important exception was represented by MDA-MB-231 cells, where a partial, although significant, reversion of the effect of cannabidiol was observed in the presence of selective antagonists for TRPV1 and CB_2 receptors, thus pointing to the partial involvement of these receptors in the anticancer action of this cannabinoid in breast carcinoma cells. This finding is important in view of the fact that these cells were the ones used in the present study to investigate the anticancer and antimetastatic effects of cannabidiol in vivo. However, the present observation that "pure" agonists of CB_2 and TRPV1 receptors, or a selective inhibitor of anandamide uptake, were less efficacious than cannabidiol at inhibiting

MDA-MB-231 cell growth strongly suggests that the two receptors act cooperatively with other mechanisms at inducing apoptosis and that other unique effects of cannabidiol also contribute to its anticancer actions.

It has been reported that plant and endogenous cannabinoids can induce apoptosis through several molecular mechanisms (Galve-Roperh et al., 2000; Jacobsson et al., 2001). When TRPV1 is involved, apoptosis is induced by mitochondrial events triggered by TRPV1-mediated calcium influx (Maccarrone et al., 2000), whereas when CB_2 receptors are involved, ceramide accumulation seems to be the most important intracellular event causing programmed cell death (Galve-Roperh et al., 2000). Our data indicate that a part of the proapoptotic effect of cannabidiol in MDA-MB-231 cells might be due to these mechanisms. However, a TRPV1- and CB_2-independent mechanism known to induce apoptosis is the rise of intracellular ROS levels, as demonstrated by the fact that nonvanilloid-, noncannabinoid receptor-mediated anandamide-induced apoptosis is prevented by antioxidant agents (Sarker et al., 2000). Hence, the effect of cannabidiol might also be attributed to ROS production. For this reason we investigated the involvement of oxidative stress in cannabidiol effects in MDA-MB-231 cells. We found that antioxidants attenuated the proapoptotic effects of cannabidiol in these cells, suggesting that this compound is indeed capable of exerting pro-oxidative properties, at least in tumor cell lines. Importantly, the extent of the effect of the antioxidants accounted for that part of cannabidiol action that was not blocked by CB_2 and TRPV1 receptor antagonists. Accordingly, cannabidiol, at the concentrations exerting antiproliferative effects, also induces a significant enhancement of ROS levels in MDA-MB-231 cells. The capability of cannabidiol to induce ROS might be surprising in view of its phenolic chemical structure, which would rather favor an inhibitory effect on oxidative stress. However, we provided here data suggesting that cannabidiol might cause ROS elevation indirectly, i.e., by elevating intracellular Ca^{2+}. Cannabidiol-induced intracellular Ca^{2+} elevation occurred in the same range of concentrations as those necessary to cause growth inhibition, was independent of TRPV1 and CB_1 and CB_2 receptor activation, and might be related to the analogous effect recently observed with THC, cannabinol and cannabidiol in T cells (Rao and Kaminski, 2006). Finally, at a submicromolar concentration, cannabidiol was also capable of inhibiting H_2O_2-induced ROS formation, similar to what observed previously in nontumor cells (Hampson et al., 1998; Iuvone et al., 2004), thus possibly explaining why also in the present study, in certain cells and at low concentrations, or with short incubation times and in cell culturing conditions in which not so many ROS are present (i.e., in the presence of serum), this compound can also produce pro-proliferative effects.

In conclusion, our data indicate that cannabidiol, and possibly *Cannabis* extracts enriched in this natural cannabinoid, represent a promising nonpsychoactive antineoplastic strategy. In particular, for a highly malignant human breast carcinoma cell line, we have shown here that cannabidiol and a cannabidiol-rich extract counteract cell growth both in vivo and in vitro as well as tumor metastasis in vivo. Cannabidiol exerts its effects on these cells through a combination of mechanisms that include either direct or indirect activation of CB_2 and TRPV1 receptors and induction of oxidative

stress, all contributing to induce apoptosis. Additional investigations are required to understand the mechanism of the growth-inhibitory action of cannabidiol in the other cancer cell lines studied here.

References

Bifulco M and Di Marzo V (2002) Targeting the endocannabinoid system in cancer therapy: a call for further research. *Nat Med* **8:**547–550.

Bifulco M, Laezza C, Valenti M, Ligresti A, Portella G, and Di Marzo V (2004) A new strategy to block tumor growth by inhibiting endocannabinoid inactivation. *FASEB J* **18:**1606–1608.

Bifulco M, Laezza C, Portella G, Vitale M, Orlando P, De Petrocellis L, and Di Marzo V (2001) Control by the endogenous cannabinoid system of ras oncogene-dependent tumor growth. *FASEB J* **15:**2745–2747.

Bisogno T, Hanus L, De Petrocellis L, Tchilibon S, Ponde DE, Brandi I, Moriello AS, Davis JB, Mechoulam R, and Di Marzo V (2001) Molecular targets for cannabidiol and its synthetic analogues: effect on vanilloid VR1 receptors and on the cellular uptake and enzymatic hydrolysis of anandamide. *Br J Pharmacol* **134:**845–852.

Bornheim LM and Grillo MP (1998) Characterization of cytochrome P450 3A inactivation by cannabidiol: possible involvement of cannabidiol-hydroxyquinone as a P450 inactivator. *Chem Res Toxicol* **11:**1209–1216.

Casanova ML, Blazquez C, Martinez-Palacio J, Villanueva C, Fernandez-Acenero MJ, Huffman JW, Jorcano JL, and Guzman M (2003) Inhibition of skin tumor growth and angiogenesis in vivo by activation of cannabinoid receptors. *J Clin Investig* **111:**43–50.

Colasanti BK (1990) A comparison of the ocular and central effects of delta 9-tetrahydrocannabinol and cannabigerol. *J Ocul Pharmacol* **6:**259–269.

Contassot E, Tenan M, Schnuriger V, Pelte MF, and Dietrich PY (2004) Arachidonyl ethanolamide induces apoptosis of uterine cervix cancer cells via aberrantly expressed vanilloid receptor-1. *Gynecol Oncol* **93:**182–188.

De Petrocellis L, Bisogno T, Davis JB, Pertwee RG, and Di Marzo V (2000) Overlap between the ligand recognition properties of the anandamide transporter and the VR1 vanilloid receptor: inhibitors of anandamide uptake with negligible capsaicin-like activity. *FEBS Lett* **483:**52–56.

De Petrocellis L, Melck D, Palmisano A, Bisogno T, Laezza C, Bifulco M, and Di Marzo V (1998) The endogenous cannabinoid anandamide inhibits human breast cancer cell proliferation. *Proc Natl Acad Sci USA* **95:**8375–8380.

Galve-Roperh I, Sanchez C, Cortes ML, del Pulgar TG, Izquierdo M, and Guzman M (2000) Anti-tumoral action of cannabinoids: involvement of sustained ceramide accumulation and extracellular signal-regulated kinase activation. *Nat Med* **6:**313–319.

Gaoni Y and Mechoulam R (1964) Isolation, structure and partial synthesis of an active constituent of hashish. *J Am Chem Soc* **86:**1646–1647.

Guzman M (2003) Cannabinoids: potential anticancer agents. *Nat Rev Cancer* **3:**745–755.

Hampson AJ, Grimaldi M, Axelrod J, and Wink D (1998) Cannabidiol and (−)Delta9-tetrahydrocannabinol are neuroprotective antioxidants. *Proc Natl Acad Sci USA* **95:**8268–8273.

Ilan AB, Gevins A, Coleman M, ElSohly MA, and de Wit H (2005) Neurophysiological and subjective profile of marijuana with varying concentrations of cannabinoids. *Behav Pharmacol* **16:**487–496.

Iuvone T, Esposito G, Esposito R, Santamaria R, Di Rosa M, and Izzo AA (2004) Neuroprotective effect of cannabidiol, a non-psychoactive component from *Cannabis sativa*, on beta-amyloid-induced toxicity in PC12 cells. *J Neurochem* **89:**134–141.

Jacobsson SO, Wallin T, and Fowler CJ (2001) Inhibition of rat C_6 glioma cell proliferation by endogenous and synthetic cannabinoids: relative involvement of cannabinoid and vanilloid receptors. *J Pharmacol Exp Ther* **299:**951–959.

Kogan NM (2005) Cannabinoids and cancer. *Mini Rev Med Chem* **5:**941–952.

Ligresti A, Bisogno T, Matias I, De Petrocellis L, Cascio MG, Cosenza V, D'Argenio G, Scaglione G, Bifulco M, Sorrentini I, et al. (2003) Possible endocannabinoid control of colorectal cancer growth. *Gastroenterology* **125:**677–687.

Maccarone M, Lorenzon T, Bari M, Melino G, and Finazzi-Agro A (2000) Anandamide induces apoptosis in human cells via vanilloid receptors: evidence for a protective role of cannabinoid receptors. *J Biol Chem* **275:**31938–31945.

Massi P, Vaccani A, Ceruti S, Colombo A, Abbracchio MP, and Parolaro D (2004) Antitumor effects of cannabidiol, a nonpsychoactive cannabinoid, on human glioma cell lines. *J Pharmacol Exp Ther* **308:**838–845.

McKallip RJ, Nagarkatti M, and Nagarkatti PS (2005) Delta-9-tetrahydrocannabinol enhances breast cancer growth and metastasis by suppression of the antitumor immune response. *J Immunol* **174:**3281–3289.

Melck D, De Petrocellis L, Orlando P, Bisogno T, Laezza C, Bifulco M, and Di Marzo V (2000) Suppression of nerve growth factor Trk receptors and prolactin receptors by endocannabinoids leads to inhibition of human breast and prostate cancer cell proliferation. *Endocrinology* **141:**118–126.

Mechoulam R, Parker LA, and Gallily R (2002) Cannabidiol: an overview of some pharmacological aspects. *J Clin Pharmacol* **42 (Suppl 11):**11S–19S.

Mimeault M, Pommery N, Wattez N, Bailly C, and Henichart JP (2003) Anti-proliferative and apoptotic effects of anandamide in human prostatic cancer cell lines: implication of epidermal growth factor receptor down-regulation and ceramide production. *Prostate* **56:**1–12.

Ortar G, Ligresti A, De Petrocellis L, Morera E, and Di Marzo V (2003) Novel selective and metabolically stable inhibitors of anandamide cellular uptake. *Biochem Pharmacol* **65:**1473–1481.

Pertwee RG (1997) Pharmacology of cannabinoid CB1 and CB2 receptors. *Pharmacol Ther* **74:**129–180.

Pertwee RG (2004) The pharmacology and therapeutic potential of cannabidiol, in *Cannabinoids* (Di Marzo V ed) pp 32–83, Kluwer Academic/Plenum Publishers, New York.

Rao GK and Kaminski NE (2006) Cannabinoid-mediated elevation of intracellular calcium: a structure-activity relationship. *J Pharmacol Exp Ther* **317:**820–829.

Robson P (2005) Human studies of cannabinoids and medicinal cannabis. *Handb Exp Pharmacol* **168:**719–756.

Ruiz L, Miguel A, and Diaz-Laviada I (1999) Delta9-tetrahydrocannabinol induces apoptosis in human prostate PC-3 cells via a receptor-independent mechanism. *FEBS Lett* **458:**400–404.

Russo E and Guy GW (2006) A tale of two cannabinoids: the therapeutic rationale for combining tetrahydrocannabinol and cannabidiol. *Med Hypotheses* **66:**234–246.

Sanchez C, de Ceballos ML, del Pulgar TG, Rueda D, Corbacho C, Velasco G, Galve-Roperh I, Huffman JW, Ramon y Cajal S, and Guzman M (2001) Inhibition of glioma growth in vivo by selective activation of the CB(2) cannabinoid receptor. *Cancer Res* **61:**5784–5789.

Sanchez C, Galve-Roperh I, Canova C, Brachet P, and Guzman M (1998) Delta9-tetrahydrocannabinol induces apoptosis in C_6 glioma cells. *FEBS Lett* **436:**6–10.

Sanchez MG, Sanchez AM, Ruiz-Llorente L, and Diaz-Laviada I (2003) Enhancement of androgen receptor expression induced by (*R*)-methanandamide in prostate LNCaP cells. *FEBS Lett* **555:**561–566.

Sarfaraz S, Afaq F, Adhami VM, and Mukhtar H (2005) Cannabinoid receptor as a novel target for the treatment of prostate cancer. *Cancer Res* **65:**1635–1641.

Sarker KP, Obara S, Nakata M, Kitajima I, and Maruyama I (2000) Anandamide induces apoptosis of PC-12 cells: involvement of superoxide and caspase-3. *FEBS Lett* **472:**39–44.

Sarnataro D, Grimaldi C, Pisanti S, Gazzerro P, Laezza C, Zurzolo C, and Bifulco M (2005) Plasma membrane and lysosomal localization of CB1 cannabinoid receptor are dependent on lipid rafts and regulated by anandamide in human breast cancer cells. *FEBS Lett* **579:**6343–6349.

Vaccani A, Massi P, Colombo A, Rubino T, and Parolaro D (2005) Cannabidiol inhibits human glioma cell migration through a cannabinoid receptor-independent mechanism. *Br J Pharmacol* **144:**1032–1036.

Walsh D, Nelson KA, and Mahmoud FA (2003) Established and potential therapeutic applications of cannabinoids in oncology. *Support Care Cancer* **11:**137–143.

Address correspondence to: Dr. Vincenzo Di Marzo, Istituto di Chimica Biomolecolare, Consiglio Nazionale delle Ricerche, Via Campi Flegrei 34, 80078 Pozzuoli, Napoli, Italy. E-mail: vdimarzo@icmib.na.cnr.it